Journal of Physics:
Conference Series

PAPER • **OPEN ACCESS**

Optimization of the Capacity Value of Wind Farms using Windfarm Cluster Control

To cite this article: U. Fechner and S. J. Watson 2026 *J. Phys.: Conf. Ser.* **3224** 032045

Journal of Physics: Conference Series **3224** (2026) 032045 doi:10.1088/1742-6596/3224/3/032045

Optimization of the Capacity Value of Wind Farms using Windfarm Cluster Control

U. Fechner[1], S. J. Watson[1]

[1]Delft University of Technology, Wind Energy Section, Faculty of Aerospace Engineering, Delft, 2629, HS, the Netherlands

E-mail: u.fechner-1@tudelft.nl

Abstract. Integrating larger amounts of wind energy into the grid would be easier if the grid operator could control the amount of wind power to match demand. Can the kinetic energy stored in the wind field be used to shift any high wind power peaks towards the demand peaks? To answer this question, FLORIDyn.jl was developed, a low-computational-cost dynamic wind farm model, and an innovative model-predictive control algorithm was used for controlling a wind farm cluster. By controlling not only one wind farm, but a wind farm cluster, it was possible to achieve time shifts in the energy delivered. The results show that by controlling the induction factor of nine turbine groups in three wind farms, it was possible to increase the power output during high demand by more than 2 % for about 30 minutes. This is a promising result, considering that no additional hardware would be required. Further research is needed to integrate a mesoscale model using more representative test case inflow conditions.

1. Introduction

In recent years, wind farm control has been identified as a key element in realizing the full potential of wind energy in a future clean and sustainable global energy system [1]. With an increasing share of wind energy in the electricity system, the LCOE (Levelized Cost of Energy) becomes less important, and the importance of the capacity value increases. The capacity value measures the effective firm capacity contribution of the plant to grid reliability [2]. Past research has focused on minimizing fatigue loads and increasing total power output of wind farm clusters by improving wake mixing [3]. However, in a future energy system with high shares of wind energy, the correlation between the power generated by the wind farms and the demand becomes more important. In this work, we propose a novel approach for controlling wind farm clusters to increase the correlation between the power generated by the cluster and the demand. This correlates with the capacity value and is achieved by controlling the induction factor of the wind turbine groups in a cluster of wind farms. The approach is based on a model predictive control (MPC) framework, which uses FLORIDyn.jl [4], a dynamic wind farm model at the farm level and a mesoscale model at the cluster level to predict total power output and optimize the control settings of the individual wind turbine groups. The original FLORIDyn model [5] was translated to Julia to achieve the required performance (more than 20 times performance increase compared to the Matlab implementation) and expanded to include an advection model. The MPC framework uses the NOMAD.jl blackbox optimization package [6], which is based on the Mesh Adaptive Direct Search (MADS) algorithm. The MPC framework was tested using hybrid simulations of a wind farm cluster comprising three wind farms with a total of more than 180 turbines. In this work, we present a test case with a power demand that is rising from a low to a high level. The wind farms are controlled to maximize the correlation between the power generated by the cluster and the demand using the induction factor of groups of turbines in each wind farm as control inputs. The results show that the proposed approach can increase the power generated during high demand by 2% over more than 30 minutes. This demonstrates the potential of wind farm cluster control to increase the capacity value of wind farms in future energy systems with high shares of wind energy.

The paper is structured as follows: Section 2 explains the methodology. The test case is then explained in detail in Section 3. In Section 4, the baseline control is explained, using collective turbine control only. Then, turbine group control is presented in Section 5. This control method offers a significant advantage over the baseline. Finally, in Section 6, conclusions are drawn, and an outlook is provided.

2. Methodology

To utilize model predictive control (MPC) for wind farm cluster control, a fast and sufficiently accurate wind farm model is required. For this purpose, the FLORIDyn.jl [4] model was developed. It is based on the FLORIDyn model [5], which was translated from Matlab to Julia and extended to include an advection model. FLORIDyn uses the Gaussian wake model of Bastankhah and Porte-Agel [7, 8] to calculate the velocity deficit and added turbulence at the turbine locations. Currently, it does not account for blockage effects or stratification, but this will be addressed in future research.

The model and the optimization software used are available under an open source license [4]. The command `include("examples/mpc_162.jl")` can be used with a Julia prompt to reproduce the results presented here. The optimization for collective turbine control required about 500 simulations, and the optimization with nine turbine groups required about 1400 simulations to converge, each taking about 2 min on a PC with a Ryzen 7950X CPU.

2.1. Assumptions

The main goal of this work is to demonstrate the maximal potential of wind farm cluster control under idealized conditions. For this reason, the following assumptions are made:

- The wind direction is constant and aligned with the largest extent of the wind farm cluster.
- The free-stream wind speed and free-stream turbulence intensity at the turbine hub height are constant over time.
- The demand profile is known in advance and is simplified to a constant value that rises to a higher constant value.
- The power coefficient of the turbines is ideal and corresponds to the Betz limit.
- The turbines can be controlled by setting the induction factor directly, without any delays or limitations.
- The wind farm operators are incentivized to cooperate.

Only if the gains that can be achieved under these idealized conditions are significant, does it make sense to relax these assumptions in future research. To relax the first two assumptions, a mesoscale model could be integrated to provide more realistic inflow conditions. To relax the third assumption, more realistic demand profiles could be used, and the uncertainty in the demand prediction could be taken into account. To relax the fourth and fifth assumptions, a more realistic turbine model could be used, and the control inputs could be limited to reflect the actual capabilities of the turbines.

3. Test case

As a test case, the Nordsee One wind farm layout with a free-stream wind speed of 8.2 m/s and a turbulence intensity of 6.2 % at turbine hub height was used. A constant wind direction, directly from the west, is assumed. The layout is repeated to simulate a cluster of three identical wind farms with ~12 km spacings in between. The wind farm cluster layout, split into nine turbine groups (three per wind farm), is shown in Fig. 1.

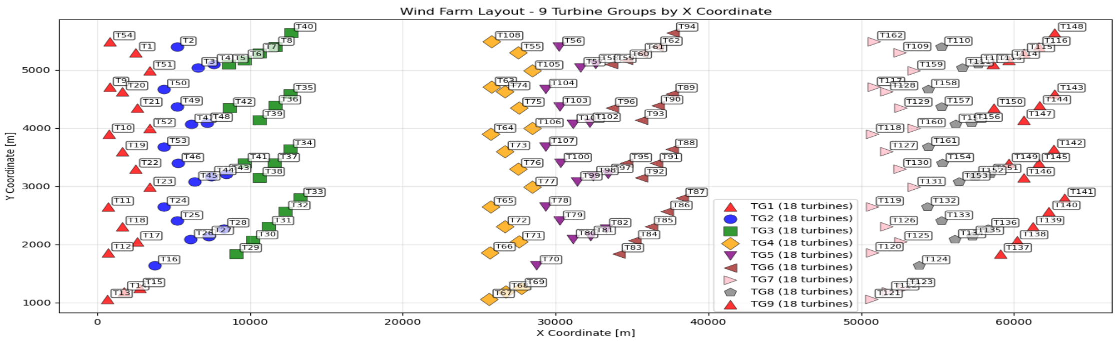

Figure 1. Wind farm cluster using three wind farms based on the Nordsee One layout. Each of the three wind farms is shown split into three groups of turbines used when implementing turbine group control (see Section 5)

The goal of optimization is to have production that matches a demand profile as closely as possible. In this test case, we assume a constant demand of 40 % of the power at free-stream wind speed at the beginning, that starts to rise at 7740 s simulation time, rises to 81 % at 8460 s and then stays constant again (see Fig. 2). The value of the final demand was chosen to match the final equilibrium power output of the wind farm cluster at the given wind speed. The start time was chosen such that the simulation starts in equilibrium, and all wakes have reached their steady state. The ramp-up time was chosen to be 12 minutes to keep the simulation time reasonable. More realistic demand profiles will be used in future research.

Fig. 2 shows the resulting relative wind farm power and relative demand as a function of time.

4. Collective turbine control

The simplest way to match production and demand is to control the induction factor of the turbines of the entire wind farm cluster, assuming all use the same induction factor.

We assume that the maximum turbine power coefficient corresponds to the Betz limit

$$C_{\mathrm{p,max}} = \frac{16}{27} \tag{1}$$

Furthermore, we assume that the relative demand (relative to the power at free-stream velocity) is given as

$$p_{\mathrm{d,rel}} = d(t) \tag{2}$$

where $d(t)$ is either the predicted demand over the time horizon of the simulation, or a simplified demand profile as described below.

The power coefficient of an ideal wind turbine at low induction factors a can be calculated as

$$C_{\mathrm{p}} = 4a(1-a)^2 \tag{3}$$

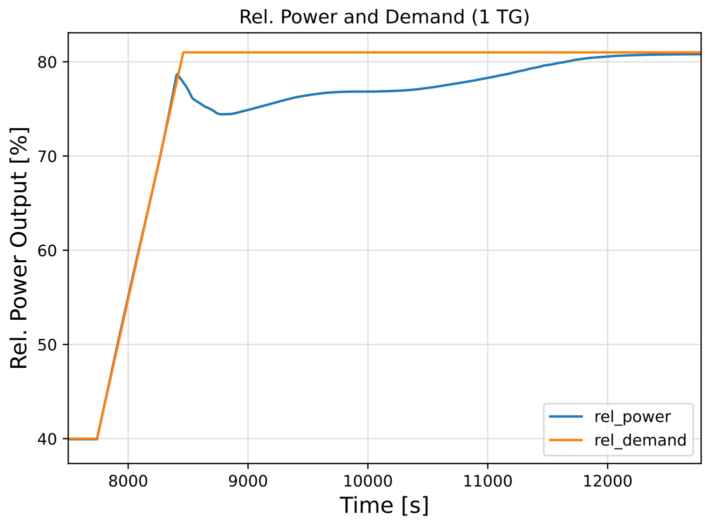

Figure 2. Relative power and demand. The figures are given relative to the output at the free stream wind velocity of 8.2 m/s. At this wind velocity, the total power output would be 810.4 MW.

The inverse relationship $a(C_{\mathrm{p}})$ is obtained by numerically solving this equation for $a \in [0, 1/3]$.

By combining Eqs. (1), (2) and (3), and applying $C_{\mathrm{p}} = d(t) \cdot C_{\mathrm{p,max}}$ we can determine the set value of the induction factor of the turbines as a function f of the demand such that

$$a = f(d(t)) \tag{4}$$

This would be correct in the absence of wakes.

4.1. Time-dependent correction factor

If the induction factor of the turbines is set according to Eq. 4, the power output of the wind farm cluster will not match the demand very well, because the downstream turbines will experience lower wind speeds due to the wakes of the upstream turbines, and thus produce less power than expected. A correction factor is needed to account for the wake losses and to ensure that the power output of the wind farm cluster matches the demand as closely as possible. If the distance between the turbines is smaller, the wake losses are higher, and thus a higher correction factor is needed.

The correction factor is defined as a smooth function of time (cubic Hermite spline, (Fageot et al. 2020)), which is optimized to minimize the difference between the power output of the wind farm cluster and the demand over the time horizon of the simulation. Control points that represent the desired correction at various time instances define the form of the spline. In this case, five control points were used to provide an acceptable resolution for the spline. The NOMAD optimizer, a black-box optimization algorithm that does not require gradient information, is used to find the optimal values of the control points.

The correction for $t \leq t_{\mathrm{start}}$ is defined by the first control point, the correction for $t \geq t_{\mathrm{end}}$ is defined by the last control point, and the additional control points are split equally between the first and last points. In the notation of mathematics:

$$c(t) = \begin{cases} c_1 & \text{if } t \leq t_{\mathrm{start}} \\ H_i(s) & \text{if } t_{\mathrm{start}} < t < t_{\mathrm{end}} \\ c_n & \text{if } t \geq t_{\mathrm{end}} \end{cases} \tag{5}$$

Journal of Physics: Conference Series **3224** (2026) 032045 doi:10.1088/1742-6596/3224/3/032045

where $s = \frac{t - t_{\text{start}}}{t_{\text{end}} - t_{\text{start}}}$ is the normalized time parameter $s \in [0, 1]$, and $H_i(s)$ is the cubic Hermite interpolation between control points c_i at positions $s_i = \frac{i-1}{n-1}$ for $i = 1, \ldots, n$.

For each segment between control points, the Hermite spline is given by:

$$H_i(s) = h_{00}(u) \cdot c_i + h_{10}(u) \cdot m_i \cdot \Delta s + h_{01}(u) \cdot c_{i+1} + h_{11}(u) \cdot m_{i+1} \cdot \Delta s \tag{6}$$

where $u = \frac{s - s_i}{\Delta s}$ with $\Delta s = \frac{1}{n-1}$, and the Hermite basis functions are:

$$h_{00}(u) = 2u^3 - 3u^2 + 1 \tag{7}$$

$$h_{10}(u) = u^3 - 2u^2 + u \tag{8}$$

$$h_{01}(u) = -2u^3 + 3u^2 \tag{9}$$

$$h_{11}(u) = u^3 - u^2 \tag{10}$$

The tangents m_i at each control point are computed using central differences:

$$m_i = \begin{cases} \frac{c_2 - c_1}{\Delta s} & \text{if } i = 1 \\ \frac{c_{i+1} - c_{i-1}}{2\Delta s} & \text{if } 1 < i < n \\ \frac{c_n - c_{n-1}}{\Delta s} & \text{if } i = n \end{cases} \tag{11}$$

To obtain the vector of the control points

$$\mathbf{c} = (c_1, \ldots, c_n) \tag{12}$$

we solve the following optimization problem using the NOMAD (Montoison et al. 2020) optimizer:

$$\min_{\mathbf{c}} \sum_{t=t_{\text{start}}}^{t_{\text{end}}+t_{\text{extra}}} (p(t) - d(t))^2 \tag{13}$$

where $p(t)$ is the wind farm cluster power output at time t relative to the power at free-flow wind speed, t_{start} is the time when the demand starts to increase, t_{end} the time when it reaches its maximum and t_{extra} the time the wind field needs to reach its equilibrium.

Fig. 3 shows optimal correction factors as a function of the time as determined by the optimizer. The curve rises when demand increases. This makes sense, because a higher demand causes higher induction factors, which cause more wake losses that need to be compensated.

If we use the correction factors in Eq. 5 to scale the effective required demand uprated for wake losses, then Eq. 4 becomes

$$a = f(c(t) \cdot d(t)) \tag{14}$$

Using this equation, we can calculate the vector of the induction factors

$$\mathbf{a} = (a_1, \ldots, a_j) \tag{15}$$

for each time step of the simulation. Fig. 4 shows optimal induction factors as a function of time as calculated by the optimizer.

Using these induction factors as input, first, these power coefficients per turbine are calculated using Eq. 3, and then the power per turbine is calculated as

$$P = 0.5\rho\ A\ C_{\text{p}}\ U^3 \tag{16}$$

where ρ is the air density, A the rotor swept area, and U the local wind speed at the turbine, taking the wakes of the upstream turbines into account. Eq. 16 is only valid below the rated

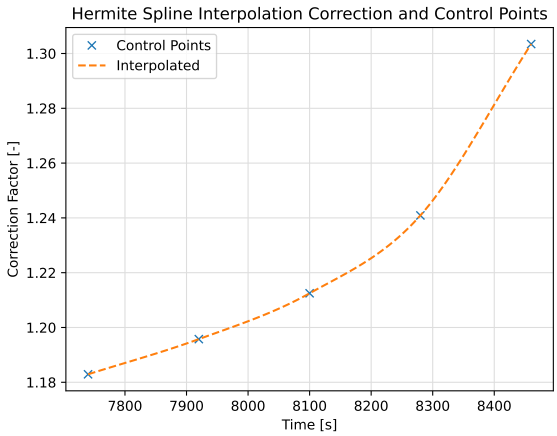

Figure 3. Correction factor for the set value of the power of the turbines

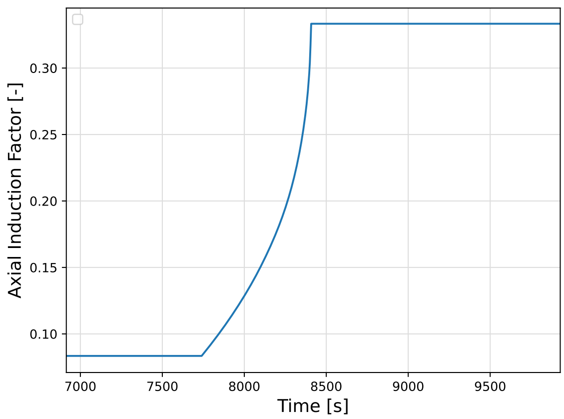

Figure 4. Induction factor, collective turbine control

wind speed of the turbines. This is no limitation, because above the rated power, there is no control strategy that can harvest additional energy. Using these formulas, the result of the FLORIDyn (Becker et al. 2022) simulation is the vector

$$\mathbf{p} = (p_1, \ldots, p_j) \tag{17}$$

of the relative wind park power (relative to the power without wakes at free-flow wind speed), where j is the number of time steps in the simulation. Fig. 2 shows the resulting relative wind park power and relative demand as a function of time. The Root Mean Square Error (RMSE) between demand and production is 3.86%.

5. Turbine group (TG) control

To improve the tracking between production and demand, the turbines are now divided into nine approximately equal-sized groups as shown in Fig. 1. The grouping is done depending on the coordinate of each turbine in the mean wind direction, such that the most upwind group of turbines has number one. Turbine group control instead of individual turbine control is used to keep the number of optimization variables manageable: For the given test case, only 9 instead of 162 induction factors need to be optimized.

The axial induction factor a of each turbine group is controlled to achieve the best match between power demand and power production. To achieve this goal, in addition to the vector $\mathbf{c}$ as defined in Eq. 12, we need a second vector that controls the power distribution of the turbine groups. We define the vector $\mathbf{e}$ with w elements as

$$\mathbf{e} = (e_1, \ldots, e_w), \quad 0 \leq e_i \leq 3 \tag{18}$$

with w being the number of turbine groups (nine in this study) and

$$e_w = \frac{3}{2}w - \sum_{i=1}^{w-1} e_i \tag{19}$$

The entries e_i are weighting factors that determine which turbine groups should add power early and which should add power later when demand goes up. When e_i is small at the beginning of the ramp, group i is asked to provide more power. When e_i is big, its contribution is delayed.

The lower limit for e_i is zero, because this means the specific turbine group always operates at full power. The upper value of three was chosen to allow a significant delay in powering up the turbine. This was found to be a suitable upper value for the given test case, which has a minimal demand of 40 %. If the minimum demand is lower, this value needs to be higher. The average of the elements in $\mathbf{e}$ is always 1.5 because the definition of e_w keeps the sum of all the entries equal to $1.5w$. The average value is just the middle of the acceptable range of $[0, 3]$, which is used here as a neutral normalization. It is not desirable on its own and does not suggest anything about future demand. With this constraint, changing $e_1..e_{w-1}$ only redistributes the requested power between the turbine groups, but does not allow the optimizer to increase or decrease all group weights at once. The variables $e_1..e_{w-1}$ are the additional free variables that need to be optimized.

The optimization problem (Eq. 13) needs to be extended to include the vector $\mathbf{e}$ and now looks like:

$$\min_{\mathbf{c},\, \mathbf{e}} \sum_{t=t_{\text{start}}}^{t_{\text{end}}+t_{\text{extra}}} \left(p(t) - d(t)\right)^2 \tag{20}$$

.

Eq. 14 must also be extended. We do this in two steps. To start, we figure out how much power each group of turbines needs to provide in relation to the others. This equation spreads the same total demand ramp over the turbine groups, but with different timing offsets. In this case, $p_{\max}$ is the highest free-stream relative power that can be given to one group of turbines. For $e_i = 0$, the turbine group must run at full power all the time. For one group, it follows the standard corrected demand signal $e_i = 1$. Higher values of e_i contribute less at the start of the ramp, and for values greater than two, the request may initially become zero, causing the turbine group to operate later. The mechanism seen later in Figs. 6 and 7 is this staggered behavior.

$$p_{\text{set,i}} = c(t)\big(p_{\max} - e_i(p_{\max} - d(t))\big) \tag{21}$$

We use the same time-dependent correction function $c(t)$ for all turbine groups, but the required relative power per turbine group is corrected using the formula given above.

The correction function based on the optimized values of $\mathbf{c}$ is shown in Fig. 5.

This value is then limited to the valid range of zero to one and is finally used to calculate the required induction factor. Using the function

$$\text{clamp}(x, a, b) = \min(\max(x, a), b) \tag{22}$$

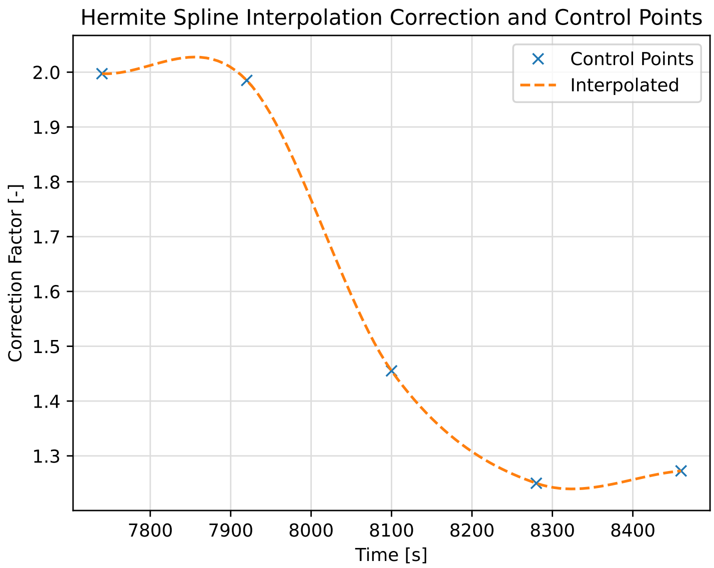

Figure 5. Correction function for nine turbine groups and five control points.

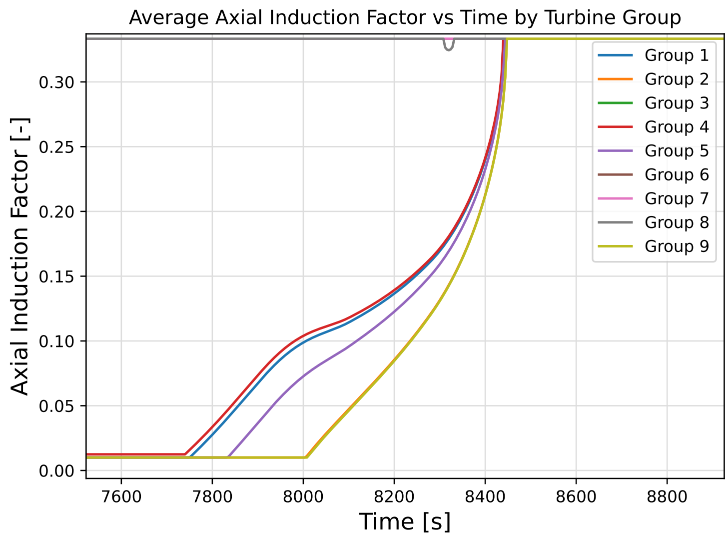

Figure 6. Induction by turbine group. Group 1 is the most upwind group. Groups 3, 6, 7, and 8 are always working on full power with an induction factor of 1/3.

we define:

$$\mathbf{a}_i = f(\mathrm{clamp}(p_{\mathrm{set,i}}, 0, 1)) \tag{23}$$

The clamp function limits the required relative power to the valid range between zero and one, which means that if the required power is negative, the turbine group operates at zero power, and if it is above one, it operates at full power. The function f is defined in Eq. 14 and is used to calculate the required induction factor based on the required relative power.

In Fig. 6, the resulting time series of the induction factors per turbine group are shown.

Using the matrix of induction factors as input, the result of the FLORIDyn (Becker et al.

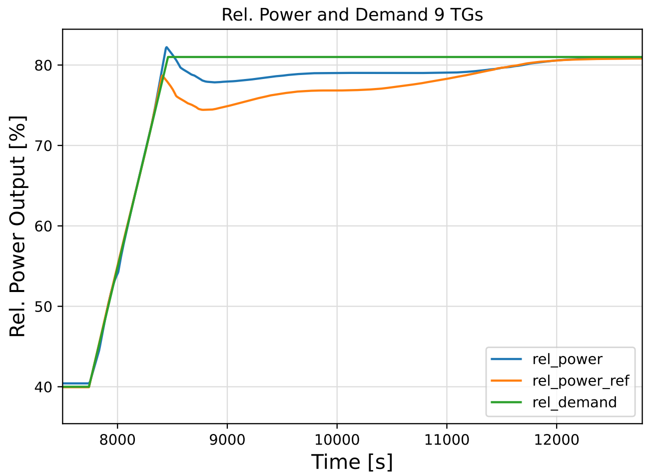

Figure 7. Relative Power and Demand, optimized result for nine turbine groups. The orange line is the reference simulation without turbine group control.

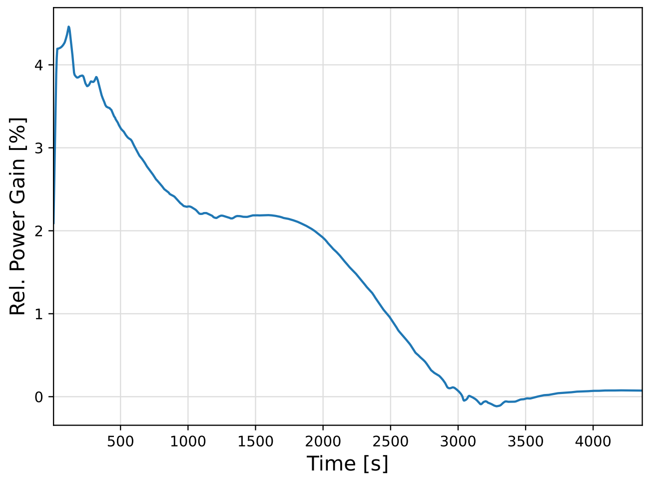

Figure 8. Relative power gain of the test case with turbine group control, compared to the reference simulation using collective induction factor control.

2022) simulation is the vector

$$\mathbf{p} = (p_1, \ldots, p_j) \tag{24}$$

of the relative wind park power (relative to the power without wakes at free-flow wind speed), where j is the number of time steps in the simulation. Fig. 7 shows the resulting relative wind farm cluster power and relative demand as a function of time.

The Root Mean Square Error (RMSE) between demand and production is 1.7 % (down from 3.31 % without turbine group control). The estimated energy storage time at 100 % power is 63.49 s. As can be seen in Fig. 8, for about 1940 s (32 minutes) more than 2 % additional power is available, compared to collective turbine control. This energy might have been stored as kinetic energy in the wind field, but it is also possible that turbulence-induced wake mixing is responsible for this gain. Further research is needed to understand the underlying physical mechanisms.

6. Conclusions and outlook

Using the FLORIDyn dynamic wake model, simulations indicate that an increase in power when it is needed most is possible, i.e. approximately 2 % more power for 32 minutes for a wind farm cluster consisting of three wind farms with 162 turbines. This represents a significant increase in capacity value, considering that no additional hardware is required to achieve this. A major contribution of this work is the development of an algorithm to reduce the number of optimization variables needed to control the induction factors of the 162 turbines to a manageable number (in this example, 13). This makes the optimization problem solvable in a reasonable time.

It should be noted that in the presented test case, the wind direction was aligned with the largest extent of the wind farm cluster, which is a favorable condition for the proposed control strategy.

Future research will focus on the following topics:

- Improving the model accuracy by tuning the model parameters to high-fidelity simulation data.
- Using different test cases with varying wind speeds and directions.
- Integrating FLORIDyn with a mesoscale model to achieve more realistic inflow conditions.

Acknowledgements

This research was funded as part of the EuroWindWakes project, the Dutch part of which received funding from RVO (contract HEP24-03681024), as part of the EU Clean Energy Transition Partnership (CETP) initiative.

References

[1] Meyers J, Bottasso C, Dykes K, Fleming P, Gebraad P, Giebel G, Göçmen T and van Wingerden J W 2022 Wind farm flow control: prospects and challenges *Wind Energy Science* **7** 2271–2306 URL https://dx.doi.org/10.5194/wes-7-2271-2022

[2] Milligan M and Porter K 2008 Determining the capacity value of wind: An updated survey of methods and implementation Conference Paper NREL/CP-500-43433 National Renewable Energy Laboratory presented at WindPower 2008, Houston, Texas, June 1–4, 2008 URL https://www.ctc-n.org/sites/default/files/resources/43433.pdf

[3] Gutknecht J, Becker M, Taschner E, Stipa S, Allaerts D, Viré A and Wingerden J W V 2024 Active cluster wake mixing *Journal of Physics: Conference Series* **2767** 092052 URL https://iopscience.iop.org/article/10.1088/1742-6596/2767/9/092052

[4] Fechner U and Becker M 2025 FLORIDyn.jl: A dynamic wind farm simulation software software URL https://doi.org/10.5281/zenodo.17121845

[5] Becker M, Allaerts D and van Wingerden J W 2022 Floridyn - a dynamic and flexible framework for real-time wind farm control *Journal of Physics: Conference Series* **2265** 032103 URL https://iopscience.iop.org/article/10.1088/1742-6596/2265/3/032103

[6] Montoison A, Pascal P and Salomon L 2020 NOMAD.jl: A Julia interface for the constrained blackbox solver NOMAD https://github.com/bbopt/NOMAD.jl

[7] Bastankhah M and Porté-Agel F 2014 A new analytical model for wind-turbine wakes *Renewable Energy* **70** 116–123 URL https://doi.org/10.1016/j.renene.2014.01.002

[8] Bastankhah M and Porté-Agel F 2016 Experimental and theoretical study of wind turbine wakes in yawed conditions *Journal of Fluid Mechanics* **806** 506–541 URL https://doi.org/10.1017/jfm.2016.595

A. Appendix

Fig. 9 shows the flow field at the beginning of the simulation, with a low demand of 40 % of the power at free-flow wind speed. The turbine groups 1, 2, 4, 5, and 9 are inactive. Fig. 11 shows the flow field at the end of the simulation, with a demand of 81 % of the power at free-flow wind speed. All turbines operate at full power. The white lines behind the turbines indicate the operation points (white dots), which are the locations where turbulence, velocity, and wind direction are calculated. These lines would be curved if the wind direction changes over time. They follow the advection of the flow field.

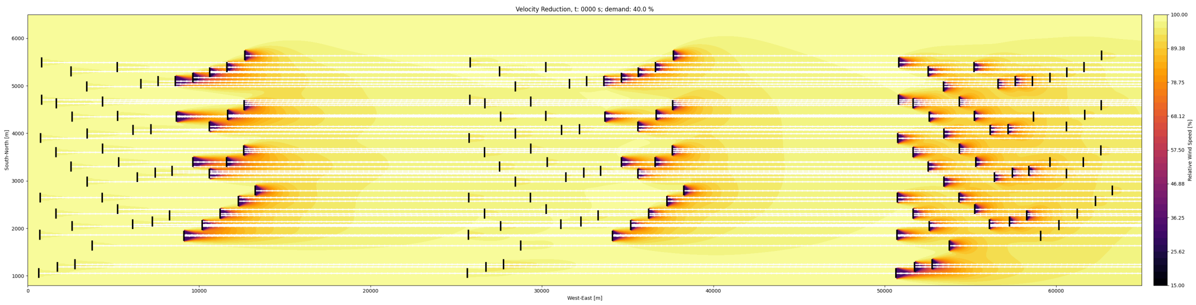

Figure 9. Flowfield at turbine height at the beginning of the simulation, after achieving steady state. The turbine groups 1, 2, 4, 5, and 9 are inactive.

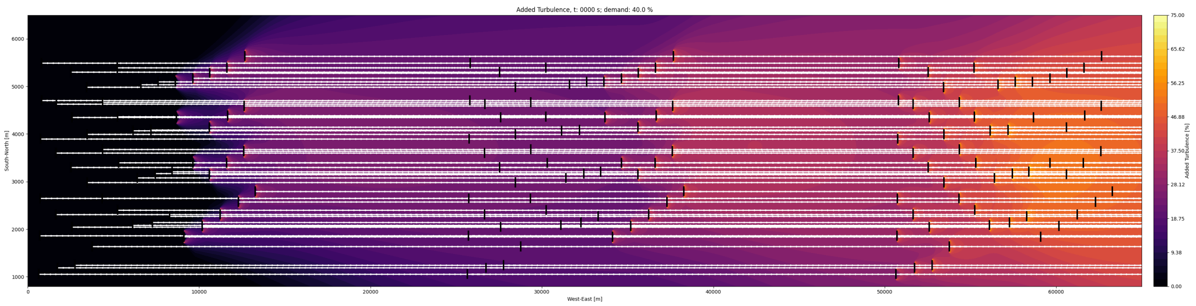

Figure 10. Added Turbulence at the beginning of the simulation, after achieving steady state. The turbine groups 1, 2, 4, 5, and 9 are inactive.

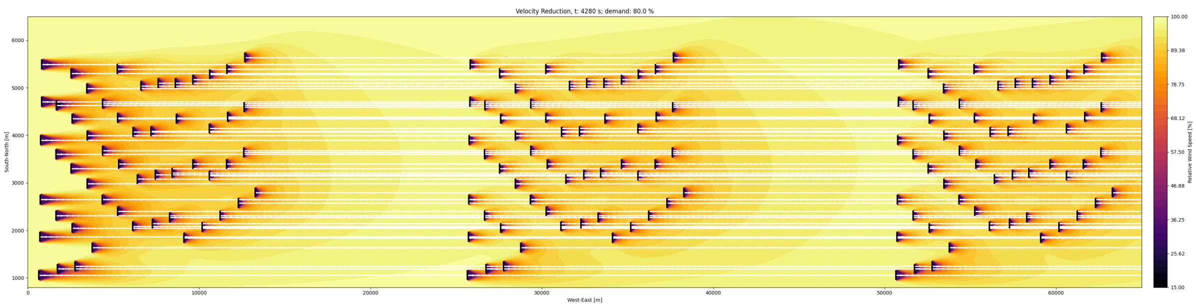

Figure 11. Flowfield at turbine height at the end of the simulation, after achieving steady state. All turbines operate at full power.